Electronic Supplementary Material (ESI) for Lab on a Chip.

Electronic Supplementary Information

Microfluidic Bead Trap as a Visual Bar for Quantitative Detection of Oligonucleotides

Zichen Zhao,[a] Yuanye Bao,[a] Lok Ting Chu,[b] John Kin Lim Ho,[a] Ching-Chang Chieng,[a] and Ting-Hsuan Chen*[a,b,c d]

[a]*Department of Mechanical and Biomedical Engineering, City University of Hong Kong, Hong Kong Special Administrative Region. E-mail: thchen@cityu.edu.hk*

[b]*School of Creative Media, City University of Hong Kong, Hong Kong Special Administrative Region*

[c]*Centre for Robotics and Automation, City University of Hong Kong, Hong Kong Special Administrative Region*

[d]*CityU Shenzhen Research Institute, Shenzhen, China.*

Materials and Methods

Materials and Reagents. The oligonucleotide sequences are shown in Table S1. The single-strand oligonucleotides, including MB155 target, biotinylated probes (MB155 Probe 1 and Probe 2), oligonucleotides with single-mismatched sequences (SNP-A, SNP-T, and SNP-C), were purchased from BGI-Tech Solutions Co., Ltd. These oligonucleotides were obtained in the form of dry powder from the manufacturer, and dissolved in tris-ethylenediaminetetraacetic acid (Tris-EDTA) buffer (Sigma Aldrich) after receiving. The GR-5 DNAzyme, consisting of two single-strand oligonucleotides, GRDS and GRE, were purchased from Integrated DNA Technologies Pte. Ltd. and BGI-Tech Solutions Co., Ltd., respectively. GRDS and GRE were obtained in the form of dry powder and dissolved in DEPC water after receiving. The Tris-HCl, EDTA, Trition X-100, Tween-20, and NaCl were purchased from Sigma Aldrich. The polystyrene microparticles (PMPs) of 15.34 μm in diameter (CP01N, Bangs Laboratories, Inc., USA) and magnetic microparticles (MMPs) of 0.36

Table S1. The sequence of single-strand oligonucleotides.

Strand name	Sequence
MB155 Probe 1	5'-/biotin/ CCCCTATCACG-3'
MP155 Probe 2	5'-ATTAGCATTAA-/biotin/-3'
MB155	5'-TTAATGCTAATCGTGATAGGGG-3'
SNP A	5'-TTAAT**A**CTAATCGTGATAGGGG-3'
SNP G	5'-TTAAT**T**CTAATCGTGATAGGGG-3'
SNP C	5'-TTAAT**C**CTAATCGTGATAGGGG-3'
GRDS	5'-TTAATGCTA ATACTCACTAT rA GGAAGAGATGATGTCTGTCGTGATAGGGG-3'
GRE	5'-ACAGACATCATCTCTGAAGTAGCGCCGCCGTATAGTGAG -3'

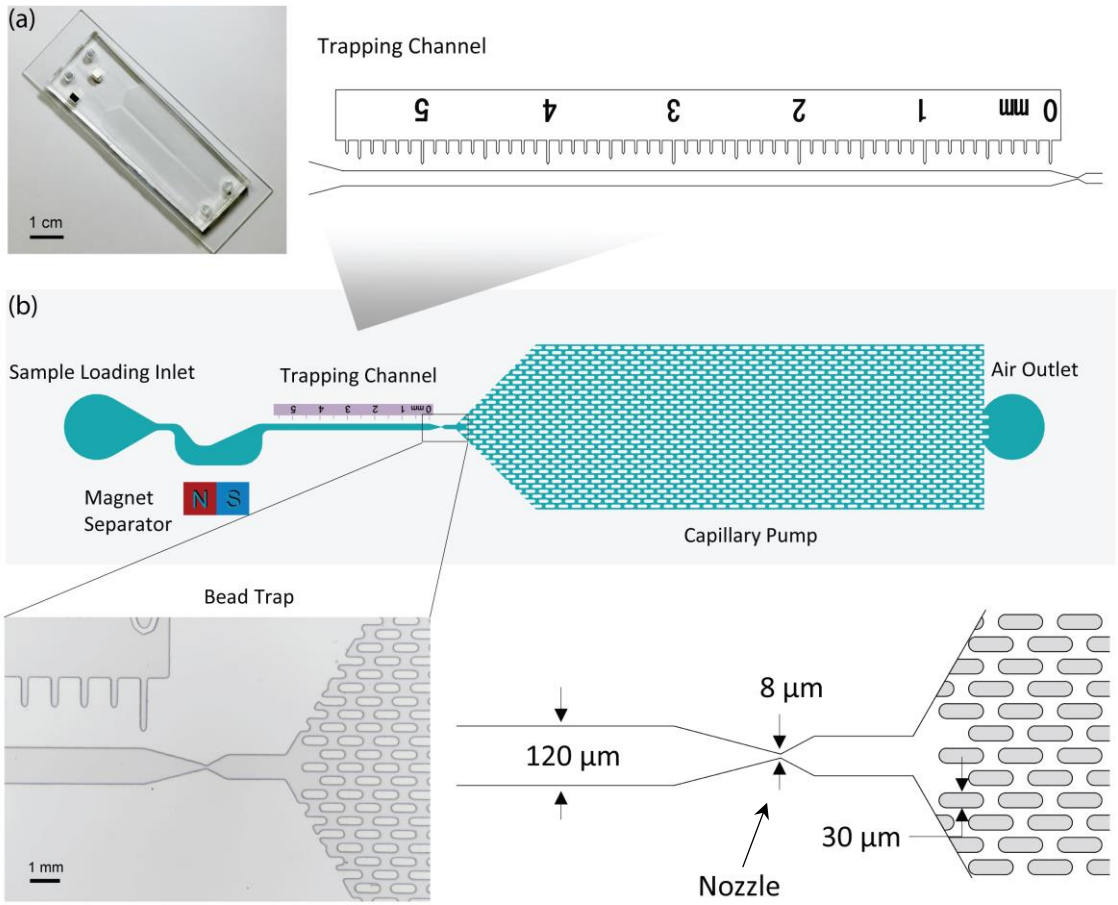

Fig. S1 Geometric design of the microfluidic device. (a) Optic image showing the overview of this device. (b) The entire system consists of a sample loading inlet, a magnetic separator, a trapping channel with a ruler, a bead trap, a capillary pump and an air outlet. The width of the trapping channel is 120 µm, and the dipstick-type ruler (upper right) has a measurement range of 5 mm. The bead trap was designed as a narrowing nozzle with the minimum width of 8 µm, which can block the PMPs with a diameter of 15.34 µm (lower left and right). The depth of the trapping channel is 25.1 ± 0.3 µm (n = 3), measured by Bruker XT Profiler, and the volume of capillary pump is 4.07 µl.

µm in diameter (CM01N, Bangs Laboratories, Inc., USA) were modified with streptavidin by the manufacturer via covalent conjugation. The polydimethylsiloxane (PDMS, Sylgard ® 184 Silicone Elastomer) was purchased from Dow Corning Corporation. The SU8-GM1070 photoresist was purchased from Gersteltec Sarl, Switzerland. The soda-lime glass slides (Sail Brand, 1" x 3") were purchased from Boshida Ltd. The magnetic field was provided by neodymium magnets in the size of 2.6 mm × 1.8 mm × 1.5 mm. All chemicals were of analytical grade. Deionized water (DI-water) was provided by a Milli-Q Plus system, with a resistivity of 18.2 MΩ·cm.

Device fabrication. The microfluidic chip was assembled by three components: a microfluidic channel, magnets, and a glass substrate. Microfluidic channel was fabricated by PDMS based soft lithography.[1] As a channel mold, one layer of SU8-GM1070 photoresist was patterned onto 3-inch silicon wafers using conventional UV-exposure photolithography. The depth of microchannel can be controlled by the thickness of the coated SU8 photoresist film at 25.1 ± 0.3 µm (n = 3). Afterward, the microchannel pattern was molded into a 3-mm thick PDMS layer. The ratio of PDMS base and curing agent was 10:1 by weight, and the curing duration was 2 hour at 70 °C. After curing, one rectangular hole of 2 mm × 3 mm was punched nearby the magnetic separator on the PDMS. Two neodymium magnets were placed into the hole in parallel. Sample loading inlet and air outlet were respectively punched with a hole with 3-mm diameter.

The microchannel and glass substrate were treated with oxygen plasma for 5 min at 800 mTorr (Harrick Plasma), followed by bonding the microchannel layer onto the glass substrate (Fig. S1).

Detection of target oligonucleotides. Briefly, 3 µl of MMPs or PMPs solution (10 mg/ml, binding capacity of 1.07 µg biotin-FITC per mg MMPs or 0.038 µg biotin-FITC per mg PMPs), was added with 3 µl of oligonucleotide probes (Probe 1 for MMPs and Probe 2 for PMPs, 100 µM). Note that both MMPs and PMPs were fully loaded as the added amount of oligonucleotides was 3 × 10^{-10} moles per particle, which is beyond the maximum loading capacity of MMPs and PMPs (3.86 × 10^{-11} mole and 1.37 × 10^{-12} mole per particle, respectively). The mixture of MMPs + Probe 1 and PMPs + Probe 2 were incubated with gently shaking for 30 min at room temperature. The residual oligonucleotides were removed by rinsing three times with 200 µl wash buffer (20 mM Tris-HCl, pH 7.5, 1 M NaCl, 1 mM EDTA, 0.0005% Trition X-100). In each washing step, MMPs were isolated using a magnetic separation rack, while the PMPs were isolated by a centrifuge (13.8 × g for 3 min). At last, the Probe 1-modified MMPs and Probe 2-modified PMPs were mixed and re-suspended in 5 µl hybridization buffer (10 mM TrisHCl, 1 mM EDTA, 1 M NaCl, 0.2% Tween 20). The target solution of 20 µl with different amount of MB155 diluted in hybridization buffer was added into the 5 µl mixture of MMPs and PMPs. To ensure adequate hybridization between oligonucleotides, the final solution was incubated for 30 min at ambient temperature with gentle vortex/shaking that keeps the microparticles monodispersed and prevents them from sinking. Thus, the sandwiched structure of "MMPs-targets-PMPs" formed, followed by loading it into the sample loading inlet of the microfluidic device. Based on the capillary force, the solution carrying PMPs and MMPs spontaneously flowed inside. At around 10 min, the region of capillary pump in the microfluidic device would be fully filled with aqueous solution and the flow stopped. The length of PMP accumulation in the trapping channel was measured via the dipstick-type ruler.

Detection of lead ion based on GR-5 DNAzyme. To prepare the GR-5 DNAzyme, the GRDS and GRE, diluted in a buffer of 50 mM Tris Acetate with 0.2 M NaCl, were first mixed at the concentration of 20 nM each for 1-hour incubation. Then, the Pb^{2+} solution of 10 µl, lead (II) acetate trihydrate diluted in DI water with different Pb^{2+}concentration, was mixed with the DNAzyme solution of 10 µl for 1 hour. Afterward, the solution of DNAzyme and Pb^{2+} of 20 µl was mixed with the solution containing mixed MMPs and PMPs of 5 µl for 30 min. Twenty µl of the final solution was thereafter loaded into our device. The remaining procedure is the same with that of the detection of target oligonucleotides.

CFD simulation and calculation of magnetic field. In the magnetic separator, the capillary flow carried the aggregates to pass through the magnetic field, during which the MMPs-targets-PMPs can be captured by the magnetic attraction. To maximize the capturing efficiency, we designed the magnetic separator as a shape of human stomach to decelerate the flow and guide the stream towards the magnets. To validate it, we used commercial CFD software package (ANYSYS, FLUENT) to model the two-dimensional, steady, single-phase flow in the magnetic separator. The calculation domain was constructed as the human stomach shape with meshes. Viscous-laminar model was selected for such incompressible, Newtonian fluid with a small Reynolds number (Re = 0.2708). The Semi-Implicit Method for Pressure-Linked Equations (SIMPLE) was used in pressure-velocity coupling. The pressure of the outlet was set as 0 Pa. A non-dimensional velocity derived by using local velocity normalized by maximum velocity was set as nominal reduced velocity. Since the depth of microchannel (25 µm) is much smaller than the size of the structure along the substrate plane, tens-of-millimeters level, two-dimensional CFD along the x-y plane was used. Experimentally, it takes around 10 min to fully fill the capillary pump (volume capacity: 4.07 µl). Thus, the velocity at the inlet can be estimated as 0.9044 mm/s. After calculation, the magnitude of flow velocity and the streamline of flow were shown in Fig. S2a-b, respectively.

The magnetic field of rectangular magnets can be determined by following formula:[2, 3]

$$\boldsymbol{B}_x(x,y,z) = \frac{\mu_0 M_s}{4\pi}\sum_{k=1}^{2}\sum_{m=1}^{2}(-1)^{k+m}\ln\left[\frac{(y-y_1)+[(x-x_m)^2+(y-y_1)^2+(z-z_k)^2]^{1/2}}{(y-y_2)+[(x-x_m)^2+(y-y_2)^2+(z-z_k)^2]^{1/2}}\right] \quad (1)$$

$$\boldsymbol{B}_y(x,y,z) = \frac{\mu_0 M_s}{4\pi}\sum_{k=1}^{2}\sum_{m=1}^{2}(-1)^{k+m}\ln\left[\frac{(x-x_1)+[(x-x_1)^2+(y-y_m)^2+(z-z_k)^2]^{1/2}}{(x-x_2)+[(x-x_2)^2+(y-y_m)^2+(z-z_k)^2]^{1/2}}\right] \quad (2)$$

where $\boldsymbol{B}_x$ and $\boldsymbol{B}_y$ are the fractions of magnet field in the direction of *x*-axis and *y*-axis, respectively, μ_0 is the vacuum permeability (4π × 10^{-7} H), M_s is a magnetization of the magnet, and (x_1, x_2), (y_1, y_2) and (z_1, z_2) denote the positions of the edges of the magnet with respect to the *x*-, *y*-, and *z*-axis, respectively. By defining the origin of this coordinate system at the center of the bottom edge of the magnetic separator, we can derive that x_1 = 1.3, x_2 = -1.3, y_1 = -0.75, y_2 = -2.55, z_1 = 0, z_2 = 3.0 mm, respectively. To estimate the value of M_s, we measured the $\boldsymbol{B}_y(0,y,0)$ along the *y*-axis using a gaussmeter (Model VGM, AlphaLab Inc., USA). The measured distances away from the magnet range from 1 mm to 10 mm at the interval of 1 mm, which corresponds to the location at the *y*-axis from 0.25 mm to 9.25 mm. Using the least-square method, we found that the M_s can be approximated as 7.84 × 10^4 A·m^{-1}, by which the calculated magnetic fields matches the experimental results. Accordingly,

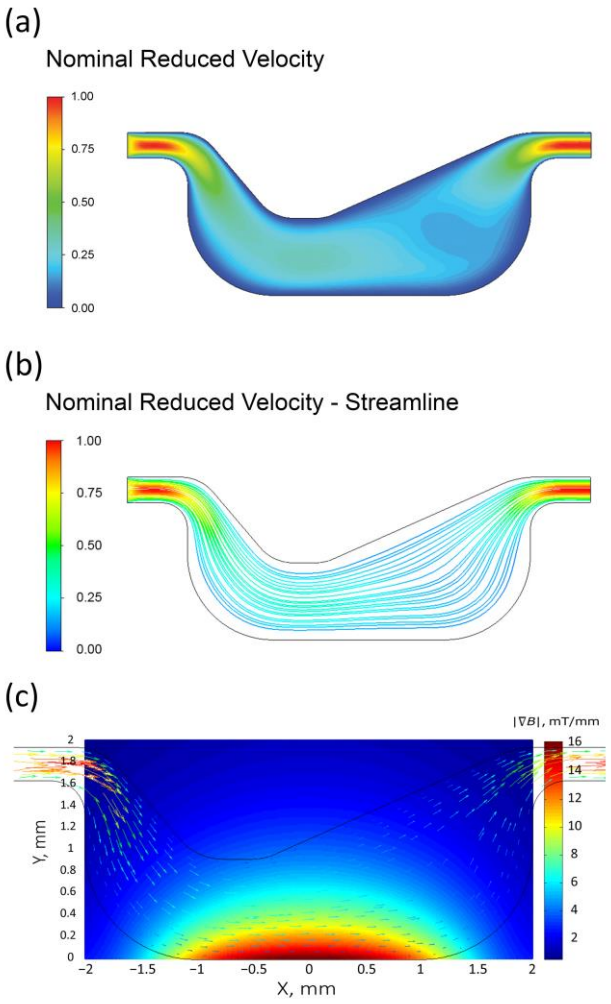

Fig. S2 CFD simulation and calculation of magnetic field. (a) The color map showing the magnitude of flow velocity in the stomach-shape microchannel. (b) Flow streamline in the stomach-shape magnetic separator using CFD simulation, where the magnitude of flow velocity was represented by the color. (c) Overlaid vector field of flow velocity and the magnetic field in the stomach-shape microchannel.

using x_1 = 1.3, x_2 = -1.3, y_1 = -0.75, y_2 = -2.55, z_1 = 0, z_2 = 3.0 mm and M_s = 7.84 × 10^4 A·m^{-1}, the gradient of magnetic field was calculated in MATLAB (Fig. S2c).

According to CFD simulation (Fig. S2a and Movie S6), we found that this structure first slows down the fluidic flow to about 30% of the maximum velocity when it flows through an expanding microchannel. Furthermore, after passing the region of strong magnetic field, the microchannel further expands, resulting in an even slower flow before leaving for the trapping channel to minimize the escaping of the aggregates of MMPs-targets-PMPs. Meanwhile, according to the streamline of flow (Fig. S2b), using a convex airfoil-type structure on the top of magnetic separator, this structure also plays a role in guiding the flow towards magnets. By overlaying the flow field and the magnetic field calculated above (Fig. S2c), we can see that the stream is guided toward the strongest region of magnetic force, which significantly enhances the capturing of the MMPs-targets-PMPs in the magnetic separator. Of note, there are only a few streamlines nearby the bottom wall of the separation region, resulting in very few unbound PMPs entering the bottom region. Moreover, even when they were near the bottom, the unbound PMPs would keep flowing laterally without aggregating with the captured MMPs (see Movie S5 and S6).

Discussion on hybridization of oligonucleotides

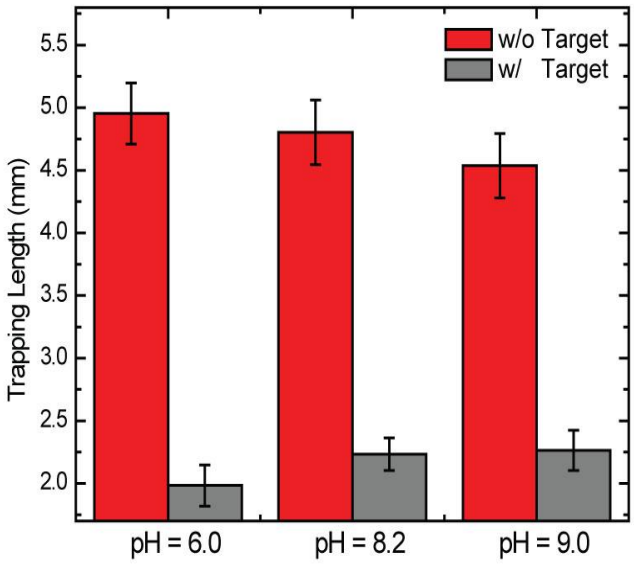

Fig. S3 Hybridization in solution with different pH values for detection of oligonucleotides. Using a sample containing target MB155 at the concentration of 200 fmol in 20 µl (w/ Target) and a blank sample (w/o Target), the trapping length showed a slight but insignificant difference with respect to different pH value (mean ± SEM, *n* = 3).

In general, the hybridization between the oligonucleotide probes and targets could be influenced by some factors such as temperature,[4, 5] ionic strength,[6-8] etc. Using IDT OligoAnalyzer Tools,[9] we analyzed temperature-induced hybridization efficiency of MB155 sequences (in solution containing 1 M Na^+ and 0.01 µM oligonucleotide). The melting temperature between MB155 Probe 1 and target oligonucleotide is 40.9 °C, and that between MB155 Probe 2 and target oligonucleotide is 28.2 °C. Those melting temperatures are above the operation temperature in our experiment (23.5 °C). Thus, by calculation, the hybridization efficiencies can be up to 100% for MB155 Probe 1 and 87.8% for MB155 Probe 2, respectively. For operation in ambient temperature, our protocol can achieve satisfactory hybridization efficiency.

We have used such hybridization-based particle assembly in various assays.[10, 11] While the particles may vary in different size (30 nm - 15.41 µm) or materials (polystyrene or gold), we found that 30 min incubation with gentle vortex/shaking, despite the vortex intensity may vary depending on different personnel, is very stable and repeatable. Similar protocol was also adopted by other researchers working on nucleic acid hybridization.[12, 13] Therefore, 30 min incubation with gentle vortex/shaking is a very reliable approach and can tolerate variations in experimental details from one to another.

Moreover, to ensure sufficient hybridization for target amount in the range of 10 fmol to 2000 fmol, we used MMPs and PMPs with the excess amount of available probes (44.77 pmol for MMPs and 1.37 pmol for PMPs). As such, it eliminates the possibility of inaccurate measurements due to insufficient capturing of target oligonucleotides.

Additionally, we also investigated the influence of pH in this hybridization process. Using target concentration of 10 nM in 20 µl (200 fmol) with pH = 6.0, 8.2 and 9.0, the result showed that as the pH values increased, the differences of trapping length between blank and target samples decreased slightly (Fig. S3). However, according to two-way ANOVA method with the confidence level of 0.05, the p-Value along with pH is 0.853. Thus, such decrease introduced by pH is not statistically significant, suggesting negligible influence by pH value.

Legends for Supplementary Movies

Movie S1. Magnetic separation for sample with MB155 target (15 X magnification).

Movie S2. Simulated particle flow along the streamline in the magnetic separator.

Movie S3. Magnetic separation for sample with MB155 target (6 X magnification).

Movie S4. PMP accumulation in a monolayer (4 X magnification).

Movie S5. Magnetic separation for blank sample without MB155 target (15 X magnification).

Movie S6. Magnetic separation for blank sample without MB155 target (6 X magnification).

References

1. Y. Xia and G. M. Whitesides, *Annu. Rev. Mater. Sci.*, 1998, **28**, 153-184.
2. E. P. Furlani, *Permanent magnet and electromechanical devices: materials, analysis, and applications*, Academic Press, San Diego, 2001.
3. K. S. Kim and J.-K. Park, *Lab Chip*, 2005, **5**, 657-664.
4. J. R. Choi, J. Hu, S. Feng, W. A. B. Wan Abas, B. Pingguan-Murphy and F. Xu, *Biosens. Bioelectron.*, 2016, **79**, 98-107.
5. C. Chen, W. Wang, Z. Wang, F. Wei and X. S. Zhao, *Nucleic Acids Res.*, 2007, **35**, 2875-2884.
6. D. Y. Zhang and E. Winfree, *J. Am. Chem. Soc.*, 2009, **131**, 17303-17314.
7. L. E. Morrison and L. M. Stols, *Biochemistry*, 1993, **32**, 3095-3104.
8. Y. Gao, L. K. Wolf and R. M. Georgiadis, *Nucleic Acids Res.*, 2006, **34**, 3370-3377.
9. R. Owczarzy, A. V. Tataurov, Y. Wu, J. A. Manthey, K. A. McQuisten, H. G. Almabrazi, K. F. Pedersen, Y. Lin, J. Garretson, N. O. McEntaggart, C. A. Sailor, R. B. Dawson and A. S. Peek, *Nucleic Acids Res.*, 2008, **36**, W163-W169.
10. Y. Li, Z. Zhao, M. L. Lam, W. Liu, P. P. Yeung, C.-C. Chieng and T.-H. Chen, *Sens. Actuator B-Chem.*, 2015, **206**, 56–64.
11. Z. Zhao, S. Chen, J. K. L. Ho, C.-C. Chieng and T.-H. Chen, *Analyst*, 2015, **140**, 7876-7885.
12. L. Lillis, D. Lehman, M. C. Singhal, J. Cantera, J. Singleton, P. Labarre, A. Toyama, O. Piepenburg, M. Parker, R. Wood, J. Overbaugh and D. S. Boyle, *PLoS One*, 2014, **9**, e108189.
13. S. Liu, Y. Lin, L. Wang, T. Liu, C. Cheng, W. Wei and B. Tang, *Anal. Chem.*, 2014, **86**, 4008-4015.